Retrieval of aerosol optical/microphysical parameters of FY-4A geostationary satellite based on Transformer

Siyu Liu[1], Lina Xu[1], Minghui Tao[2], Xincai Chang[1], Huang Zhang[1], Jianxin Ling[1], Dandi Liao[1]

[1] Hubei Subsurface Multi-scale Imaging Key Laboratory, School of Geophysics and Geomatics, China University of Geosciences, Wuhan, 430074, China

[2] Hubei Key Laboratory of Regional Ecology and Environmental Change, School of Geography and Information Engineering, China University ofGeosciences, Wuhan, 430074, China

Keywords: FY-4A, Transformer, Geostationary satellite, Aerosol optical/microphysical parameters.

Abstract

Atmospheric aerosols are a key factor influencing the Earth's radiation balance and climate change, and the accuracy of their retrieval is crucial for environmental monitoring and climate research. FY-4A AGRI, with its high-frequency observation capability, can provide aerosol data at high temporal resolution. Combined with deep learning technology, it enables efficient monitoring of dynamic aerosol variations. This study develops a retrieval algorithm for aerosol optical and microphysical parameters based on the Transformer deep learning model, specifically designed for the FY-4A geostationary satellite. The algorithm achieves multi-parameter collaborative retrieval of aerosol optical depth (AOD), fine/coarse-mode aerosol optical depth (FAOD/CAOD), and single scattering albedo (SSA). This research overcomes the reliance on prior assumptions inherent in traditional physical retrieval methods. By integrating multi-band spectral features, geometric observation parameters, and data from 104 AERONET sites, it significantly enhances retrieval accuracy under the complex surface conditions of East Asia. Experimental results demonstrate high accuracy in validation against AERONET sites, with correlation coefficients of R=0.915 for AOD, R=0.897 for FAOD, R=0.851 for CAOD, and R=0.536 for SSA. Comparative validation of various aerosol product spatial distributions highlights the advantages of the proposed algorithm in capturing aerosol diurnal variations (such as haze dissipation processes) and extreme events (e.g., dust storms and biomass burning). This study provides a new technical approach for regional air quality monitoring and climate effect assessment, advancing the application of China’s geostationary meteorological satellites in aerosol monitoring.

1. Introduction

Atmospheric aerosols directly influence the Earth's radiation budget by scattering and absorbing solar radiation, representing one of the most uncertain components in the climate system(Legg 2021). Ground-based observations can measure the optical and microphysical properties of aerosols, providing high precision and high frequency monitoring of aerosol characteristics. However, their limited global coverage prevents large-scale aerosol monitoring.

Satellite remote sensing, with its advantage of extensive coverage, has become a crucial means of monitoring aerosols(Barnaba and Gobbi 2004, Levy, Remer et al. 2007, Tao, Chen et al. 2015). Polar-orbiting satellite sensors can provide extensive continuous observations, but with only 1-2 daytime overpasses, they are insufficient in capturing the diurnal variation characteristics of aerosols. In contrast, geostationary satellites offer observation frequencies as high as hourly or even minutely levels, providing significant advantages for aerosol monitoring. Fengyun-4A (FY-4A) is the first satellite of China's second-generation geostationary meteorological satellites, equipped with the Advanced Geosynchronous Radiation Imager (AGRI) (Yang, Zhang et al. 2017). The AGRI full-disk observation mode has a temporal resolution of approximately 15 minutes, enabling the acquisition of near-real-time daytime atmospheric aerosol conditions.

As the primary payload of China's new-generation Fengyun-4 (FY-4A) geostationary meteorological satellite, the development and application of aerosol retrieval algorithms for the AGRI (Advanced Geosynchronous Radiation Imager) have garnered significant attention. Current research has primarily focused on traditional look-up table (LUT) methods for retrieving aerosol parameters(Xu, Bao et al. 2020, Jiang, Xue et al. 2022, Yanqing, Zhengqiang et al. 2022, Su, Wang et al. 2023, Si, Gao et al. 2024, Zhou, Wang et al. 2024, Wang, Fan et al. 2025). While these methods can meet aerosol monitoring requirements to a certain extent, they suffer from significant errors over complex land surfaces and in high-albedo regions due to their reliance on simplified assumptions and fixed aerosol models. Recent studies utilizing deep learning for aerosol parameter retrieval have already made considerable progress(Ding, Zhao et al. 2022, Fu, Shi et al. 2024). Aerosol data from sun photometer sites (AERONET + SONET) have been used to train neural networks for retrieving full-disk aerosol data from FY-4 AGRI. While this approach has achieved aerosol optical depth (AOD) retrieval, the retrieval accuracy ($R < 0.8$) is significantly lower than that of look-up table (LUT) methods. Moreover, it retrieves only the AOD parameter, with limited accuracy for component parameters such as fine/coarse-mode AOD (FAOD/CAOD) and microphysical parameters like single scattering albedo (SSA). To address these limitations, this study develops a comprehensive retrieval algorithm system for FY-4 AGRI geostationary satellite aerosol optical and microphysical parameters, centered on the Transformer algorithm. This system aims to provide algorithmic and technical support for research in climate change and atmospheric environment monitoring.

2. Satellite and ground measurement

2.1 FY4A measurement

FY-4A was launched on December 11, 2016, and is positioned in a geostationary orbit at 104.7°E. It began operational service as a meteorological satellite on September 25, 2017(Yang, Zhang et al. 2017). The FY-4A AGRI (Advanced Geosynchronous Radiation Imager) is equipped with 14 spectral bands covering a wavelength range from 0.45 to 13.8 μm. It provides a spatial resolution of 1 km at nadir for the visible (VIS) band, 2 km for the near-infrared (NIR) band, and 4 km for the remaining infrared spectral bands(Lu, Zhang et al. 2017, Min, Wu et al. 2017). The AGRI full-disk observation mode has a temporal resolution of approximately 15 minutes, with observations over Central and East Asia every 5 minutes,

enabling the provision of high-temporal-resolution aerosol monitoring data for China and its surrounding regions.

This study obtained the AGRI/FY-4A Level 1 (L1) dataset with a 15-minute temporal resolution and 4 km spatial resolution, along with the corresponding GEO positioning data (also at 4 km spatial resolution) for the year 2018 from the National Satellite Meteorological Center (NSMC) of China. However, due to variations in solar zenith angle, data from all time slots are not suitable for aerosol retrieval(Yanqing, Zhengqiang et al. 2022). Only the hourly data from 0:30 to 7:30 UTC were utilized. The digital number (DN) values were converted to top-of-atmosphere (TOA) radiance using a radiometric calibration algorithm. Pixel-level latitude and longitude corrections were then applied based on the FY-4A GEO positioning files, resulting in the generation of TOA reflectance datasets for Bands 1–6, along with solar and satellite geometric angle datasets (including Satellite Azimuth, Satellite Zenith, Sun Azimuth, and Sun Zenith). This study further incorporated the calculation of the Relative Azimuth Angle (RAA) to impose constraints on pixel locations for enhanced accuracy. Additionally, 1 km resolution zonal Digital Elevation Model (DEM) data, downloaded directly from NOAA, was utilized as auxiliary data.

2.2 AERONET measurement

AERONET is an aerosol observation network that retrieves aerosol optical properties through automated sun photometer measurements of direct solar radiation and sky radiance signals(Holben, Eck et al. 1998). Currently, there are over 800 stations distributed across major countries and regions worldwide, providing near-continuous daytime measurements of solar spectral irradiance, spectral AOD, water vapor, and retrieved aerosol products.

This study utilized data from 104 sites, spanning different surface types and emission sources, including both Level 2.0 and Level 1.5 data. The dataset comprises four aerosol parameters: AOD, fine and coarse AOD (FAOD and CAOD), and single scattering albedo (SSA). A combination of Level 2.0 and Level 1.5 data was employed. The AOD at 550 nm was derived using a quadratic polynomial interpolation method applied to the corresponding values at 440, 675, 870, and 1020 nm.

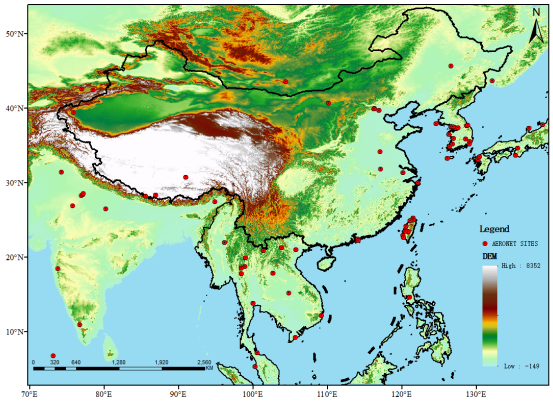

Figure 1. Distribution of AERONET sites in the study area

2.3 Other measurement

Himawari-8(H8), a new-generation geostationary satellite officially launched in July 2015, also employs a universal algorithm developed by its official team to retrieve aerosol properties for various satellite sensors over both land and ocean surfaces(Yoshida, Kikuchi et al. 2018). To maintain temporal consistency with the FY-4A data (15-minute resolution) used in this study, the JAXA H8 Level 2 products—with a temporal resolution of 10 minutes and a spatial resolution of 5 km—were employed for comparative validation of aerosol optical depth (AOD) products.

The Moderate Resolution Imaging Spectroradiometer (MODIS) Level 2 aerosol product (MOD04/MYD04), derived from the Terra/Aqua satellites' MODIS L2 aerosol data (10 km resolution), provides prior information such as aerosol types (e.g., continental, dust) and fine-mode fraction (Zhang and Reid 2006). This study selected the AOD (550 nm) retrieved by the Dark Target (DB) algorithm from the MOD04_L2 dataset as the comparative validation dataset.

3. Research methodology

3.1 Data preprocessing

Based on a land clear-sky aerosol retrieval algorithm, this study first applies the FY-4A/CLM cloud product dataset to perform cloud masking on the satellite observations, screening "Clear"-grade cloud-free pixels to obtain observational data under cloudless conditions.

Subsequently, the FY-4A satellite observations are spatiotemporally matched with the AERONET ground-based aerosol measurements. Since AERONET provides continuous observations at discrete sites at fixed time intervals, while FY-4A captures instantaneous observations with a certain spatial resolution, a temporal window of ±30 minutes is set during the matching process, and multi-temporal satellite observations within this period are averaged. Spatially, a 3×3 pixel window matching algorithm is adopted. This process establishes a training sample set linking FY-4A's TOA reflectance with AERONET aerosol optical depth (AOD) data(She, Zhang et al. 2020, Cao, Zhang et al. 2023).

Finally, based on the spatiotemporally matched training dataset, the subsequent model training was conducted using the following as model inputs: TOA reflectance from five visible-to-near-infrared bands (Band 1: 0.47μm, Band 2: 0.65μm, Band 3: 0.825μm, Band 5: 1.61μm, Band 6: 2.225μm), five geometric observation parameters (SZA, VZA, SAA, VAA, RAA), and DEM. Figure 2 shows the flowchart of this study.

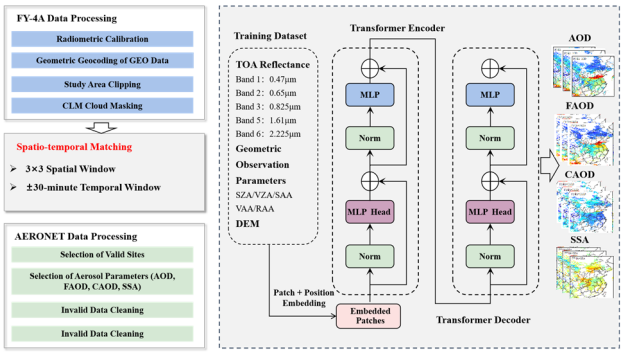

Figure 2. Technical Flowchart

3.2 Transformer Model

The Transformer model applys an encoder-decoder architecture to retrieve aerosol properties(Lundberg and Lee 2017, Vaswani, Shazeer et al. 2017). The encoder incorporates a multi-head self-attention mechanism to automatically learn long-range dependencies among multi-band spectral features. It also employs residual connections and layer normalization to prevent gradient vanishing and enhance training stability. The decoder

integrates AERONET label data to output target parameters (AOD, FAOD/CAOD, SSA), utilizing an attention mechanism to focus on key features(Wei, Chang et al. 2020, Wei, Wang et al. 2024). The regularization design incorporates Dropout layers to prevent overfitting, ensuring the model's generalizability over complex surfaces (e.g., urban, desert). A fully connected layer maps the decoder outputs to specific parameter values, generating AOD, FAOD/CAOD, and SSA.

A two-stage hierarchical training strategy is implemented: the first stage employs unsupervised pre-training to learn representations of aerosol scattering characteristics. The second stage involves transfer learning fine-tuning, where a backpropagation neural network is introduced to adjust the model via backpropagation, addressing domain shift issues under complex surface conditions in East Asia(Jiang, Tao et al. 2023). From the sample dataset, 80% is randomly selected as training samples for model development, generating the Transformer-based retrieval model, while the remaining 20% is reserved as test samples for model evaluation(Hilborn, Catanzaro et al. 2012). Performance is validated using the correlation coefficient (R), mean absolute error (MAE), root mean square error (RMSE), and expected error (EE).

$$R = \frac{\sum_{i=1}^{n}(x_i - \overline{x})(y_i - \overline{y})}{\sqrt{\sum_{i=1}^{n}(x_i - \overline{x})^2}\sqrt{\sum_{i=1}^{n}(y_i - \overline{y})^2}} \quad (1)$$

$$MAE = \frac{1}{n}\sum_{i=1}^{n}|y_i - \hat{y}_i| \quad (2)$$

$$RMSE = \sqrt{\frac{1}{n}\sum_{i=1}^{n}(y_i - \hat{y}_i)^2} \quad (3)$$

$$EE = \pm(0.05 + 20\% * \hat{y}_i) \quad (4)$$

4. Results and analysis

4.1 *Ground validation of FY4A aerosol retrievals*

To evaluate the performance and robustness of the Transformer model at a regional scale, we analyzed the annual mean FY-4A aerosol retrievals for 2019 and conducted intercomparisons with MODIS aerosol products and the official JAXA H8 product. The validation over Eastern China was performed by comparing the annual averages of aerosol parameters derived from FY-4A and JAXA H8 hourly data (from 0:30 to 7:30 UTC) with the annual mean of the MOD04_DB product (Figure 3).

Both FY-4A AOD and FAOD show exceptionally high correlation with AERONET observations (R = 0.915 and 0.897, respectively), accompanied by relatively low root mean square errors (RMSE = 0.135 and 0.148). FY-4A CAOD also achieves reliable performance (R = 0.851, RMSE = 0.065). The slightly reduced accuracy of CAOD may be attributed to weaker backscattering signals and lower information content associated with coarse-mode particles. FY-4A SSA at 440 nm exhibits consistent variation with AERONET retrievals (R = 0.536, RMSE = 0.049).

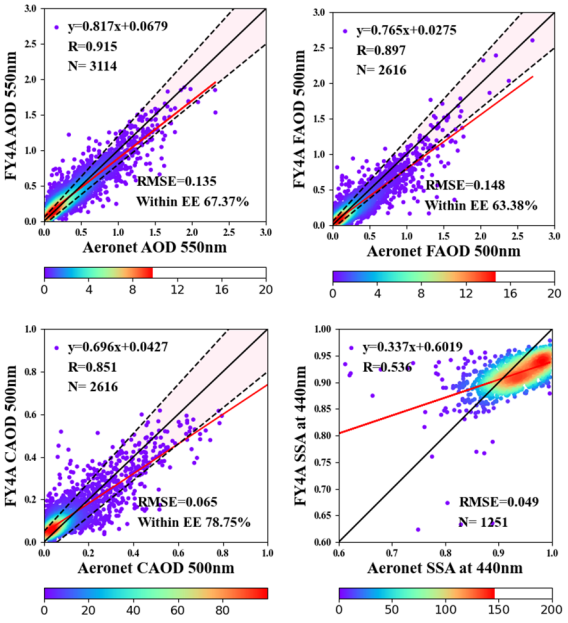

Figure 3. Scatter plots of the retrieved AOD (550 nm), FAOD/CAOD (500 nm), and SSA (440 nm) against the corresponding AERONET AOD, FAOD, CAOD, and SSA measurements.

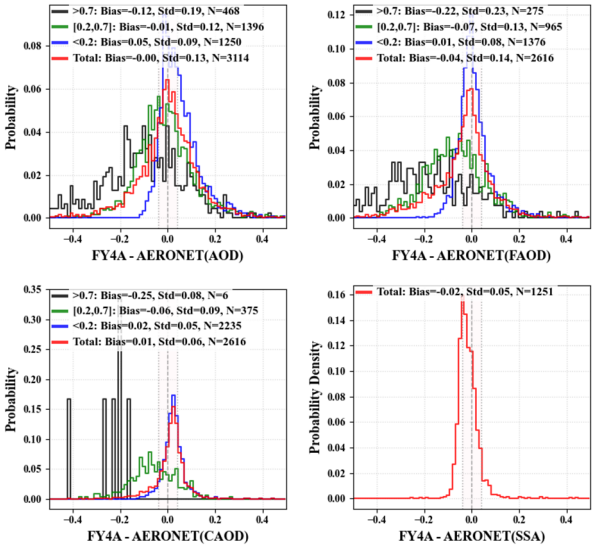

Figure 4. Scatter plots of the retrieved AOD (550 nm), FAOD/CAOD (500 nm), and SSA (440 nm) against the corresponding AERONET AOD, FAOD, CAOD, and SSA measurements.

The probability density functions of the deviations between FY-4A retrieved AOD, FAOD, CAOD, SSA and AERONET observations indicate that the total samples (red curve) follow an approximately normal distribution. The bias and standard deviation values suggest no significant systematic bias in the FY-4A retrieval system, though moderate dispersion is present. The significant negative bias (-0.25) in FY-4A CAOD indicates a substantial systematic underestimation of coarse-mode aerosol concentrations, particularly at high values. Within the high-concentration range (AOD > 0.7, black curve), the extremely limited number of samples (N=6) reflects the scarcity of data for

desert/dust scenarios, highlighting the need for improved retrieval capability for intense dust events.

4.2 *Inter-comparison with Other Aerosol Retrievals*

This study spatially evaluates the FY-4A retrieval performance by comparing the annual mean from JAXA H8 and FY-4A Transformer (00:30–07:30 UTC, 2019) with the annual average from MODIS Deep Blue (all daytime overpasses). As shown in Figure 5, the annual mean for 2019 derived from the FY-4A Transformer model shows a highly consistent distribution with the MODIS DB product. Compared to JAXA AOD and MODIS AOD, the FY-4A retrieval results exhibit a consistent spatial distribution but offer enhanced capability in highlighting emission sources in some eastern regions. Furthermore, FY-4A FAOD, CAOD at 500 nm, and SSA at 440 nm demonstrate good self-consistency. The hotspots of FY-4A FAOD are concentrated in urban/industrial areas, while the high values of CAOD are primarily located in the Gobi Desert.

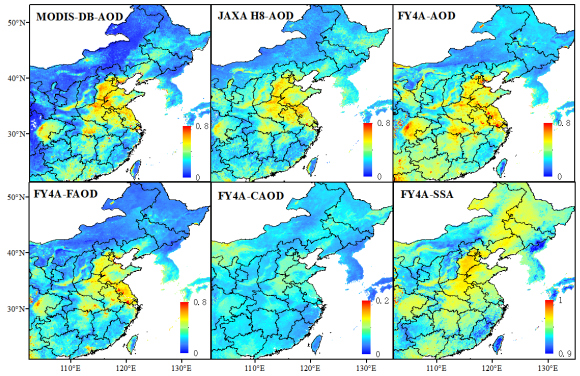

Figure 5. Comparison of annual mean aerosol products.

As shown in Figure 6, the MODIS true-color image from 6 April 2019 reveals a distinct banded haze episode over eastern China, particularly evident in regions such as Hubei and Shandong. Consistent with these observations, the FY-4A retrievals show significantly increased AOD and FAOD values with clear spatial patterns, indicating that anthropogenic fine particulate matter is the dominant contributor to the haze formation.

In the desert and plateau regions of Inner Mongolia, CAOD exhibits high values, consistent with the dominance of natural aerosol sources (e.g., dust aerosols) in this area. The FY-4A retrieval results further verify that aerosols in this region are predominantly coarse-mode, contrasting with the pollution characteristics of eastern China, which are primarily influenced by anthropogenic fine particles.

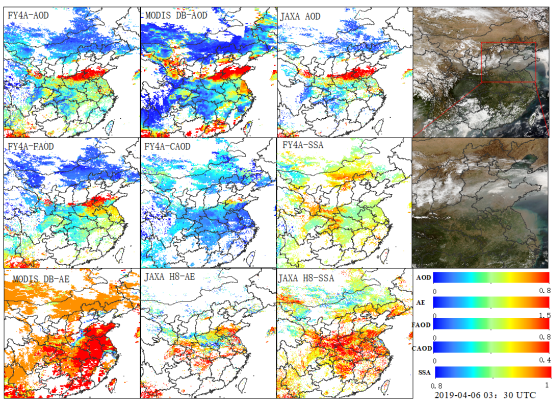

Figure 6. Haze case on 6 April 2019 (03:30 UTC).

A comparative analysis based on the MODIS true-color image and FY-4A AOD retrieval results from April 13, 2018, reveals significant biomass burning smoke plumes over Southeast Asia (Figure 7). The FY-4A AOD retrievals show good consistency with MODIS and JAXA AOD products. However, due to the spatiotemporal resolution limitations of the polar-orbiting MODIS observations, its retrieval results exhibit strip-like data gaps, while the JAXA data contains extensive spatial voids.

Aerosols in this region are predominantly fine-mode particles. The FY-4A FAOD product effectively characterizes the distribution of fine particulate aerosols, while CAOD values remain low. Although the Ångström Exponent (AE) can indicate aerosol size distribution, the accuracy of AE products from both MODIS and JAXA is limited, making it difficult to accurately reflect the aerosol particle size characteristics in Southeast Asia. The FY-4A SSA product illustrates the aging process of the smoke plumes. As the air mass transports away from the pollution source, the aerosols undergo aging, leading to an increase in SSA values. This phenomenon aligns with the change in optical properties where light-absorbing components diminish during aerosol aging.

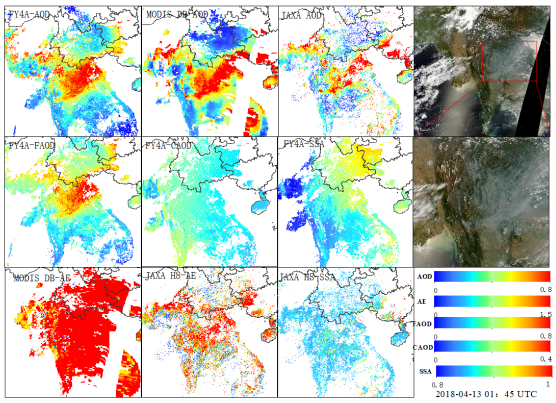

Figure 7. Biomass burning case on 13 April 2018 (01:45 UTC).

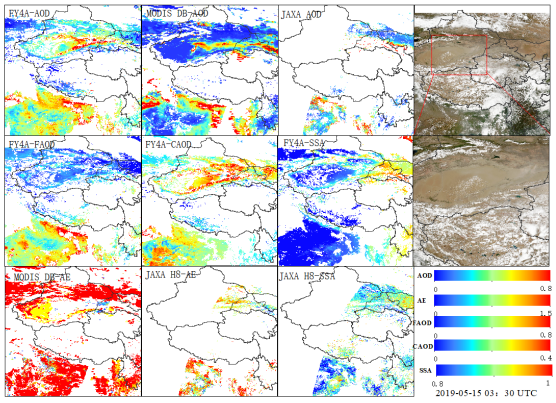

Figure 8. Dust case on 15 May 2019 (03:30 UTC).

As shown in Figure 8, a significant dust pollution event was recorded in the Xinjiang region on May 15, 2019. MODIS true-color imagery clearly revealed the transport pathway and spatial distribution characteristics of the dust aerosols. Both the FY-4A and MODIS AOD products effectively captured the dust pollution conditions in the area. Benefiting from its high spatiotemporal resolution, the FY-4A product more completely

This contribution has been peer-reviewed. The double-blind peer-review was conducted on the basis of the full paper.
https://doi.org/10.5194/isprs-annals-XI-3-2026-649-2026 | © Author(s) 2026. CC BY 4.0 License.

depicted the temporal evolution and spatial spread of the dust event. In contrast, limited by its observational coverage, the JAXA AOD product failed to provide complete spatial coverage of this dust event.

The CAOD product effectively characterizes the distribution of coarse-mode aerosols, such as dust. The FY-4A CAOD product clearly illustrated the spatial pattern of coarse-mode aerosols during this event, with areas of high CAOD values aligning closely with the dust transport pathway. The FAOD product showed a weaker response to the dust aerosols, consistent with the physical characteristic of dust being predominantly composed of coarse particles. Across the affected region, Ångström Exponent (AE) values from both MODIS and JAXA were generally below 1.0, further confirming the dominance of coarse-mode aerosols in this pollution episode. However, due to accuracy limitations, the AE products did not clearly represent the spatial distribution of this dust event.

Based on high spatiotemporal resolution observations from FY-4A, a significant haze dissipation process was observed on March 23, 2018(Figure 9), extending from the North China Plain (Hebei) to the middle and lower reaches of the Yangtze River (Hubei, Anhui, Jiangsu). At 00:45 UTC (08:45 Beijing Time), the haze coverage reached its maximum extent, with AOD values generally exceeding 1.0 and visibility dropping below 5 km. The haze subsequently weakened hourly, and by 06:45 UTC (14:45 Beijing Time), the AOD had decreased by 30%–50%, with a notable contraction in its spatial coverage.

This dissipation process was closely associated with the rise of the planetary boundary layer after sunrise, a decrease in relative humidity, and the dispersive effect of local weak easterly winds. FY-4A observations indicated that the clearance rate of FAOD was faster than that of CAOD, leading to a temporal evolution in aerosol size distribution. The SSA increased from 0.92 to 0.95, reflecting aerosol aging characteristics. This case highlights the unique advantage of geostationary satellites in capturing the dynamic evolution of haze processes.

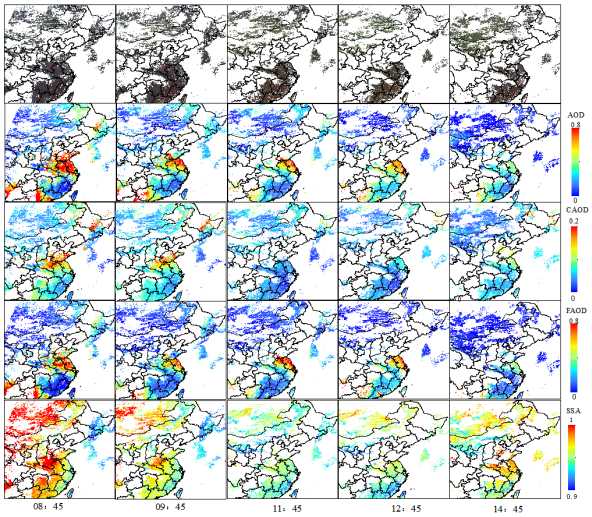

Figure 9. Hourly haze case from 23 March 2018 (00:45 to 06:45 UTC).

5. Conclusions

Atmospheric aerosols significantly impact the Earth-atmosphere system, radiation balance, and atmospheric environment. However, due to their short lifecycle and strong spatiotemporal variability, the temporal resolution of polar-orbiting satellite sensors can no longer meet monitoring requirements. To study the dynamic changes and regional characteristics of aerosols, this study utilizes high-temporal-resolution geostationary satellite data to propose a Transformer-based FY-4A aerosol retrieval algorithm, enabling large-scale, minute-level retrieval of aerosol parameters. The main work and conclusions of this study are as follows:

(1) Through the processing of FY-4A data, cloud-free TOA reflectance data for Bands 1-6 and solar/satellite geometric angle datasets were obtained. A spatiotemporal matching process using a 3×3 pixel sampling window centered on the coordinates of corresponding AERONET sites was applied to create the training and testing datasets.

(2) The Transformer model successfully retrieved AOD, FAOD, CAOD, and SSA with high accuracy, with most results falling within the expected error limits. The correlation coefficients (R) were 0.915 for AOD, 0.897 for FAOD, 0.851 for CAOD, and 0.536 for SSA. These validation results demonstrate the high precision and reliability of the proposed algorithm, showing improvement over previous research achievements.

(3) The aerosol model was applied, and the retrieval results showed consistency with the true-color imagery from the corresponding days. Analysis of the aerosol parameter distributions indicates that fine-mode aerosols from anthropogenic emissions are the primary cause of severe haze in eastern China, while natural coarse-mode aerosols dominate in desert regions. The retrieval results provide valuable information for air quality monitoring and assessment in eastern China. A comparison between the Transformer model results and MODIS aerosol products, as well as the official JAXA H8 product, confirms that the proposed model can provide stable and continuous spatial aerosol distribution results over eastern China.

The model presented in this study demonstrates high accuracy and applicability. It can not only reveal the large-scale distribution of aerosols but also provide important insights into spatiotemporal variations at smaller regional scales, contributing to a better understanding of aerosol sources, distribution, and impacts. Compared to traditional methods, the proposed algorithm offers significant advantages. It requires only single-phase satellite remote sensing data for aerosol optical depth retrieval, eliminating the need for complex physical modeling and thus simplifying the inversion process. More importantly, this method effectively improves retrieval accuracy and extends the capability to retrieve challenging aerosol parameters such as FAOD and CAOD.

Acknowledgements

We gratefully acknowledge the use of FY-4A data from the National Satellite Meteorological Center (NSMC) of China, Himawari-8 data from the Japan Meteorological Agency (JMA), MODIS data from the NASA Level-1 and Atmosphere Archive & Distribution System (LAADS) Distributed Active Archive Center (DAAC), and AERONET data from the National Aeronautics and Space Administration (NASA). This research was funded by the 2025 University Student Independent Innovation Funding Program (Grant No. 2025XLA177).

References

Barnaba, F. and G. Gobbi. 2004: Aerosol seasonal variability over the Mediterranean region and relative impact of maritime, continental and Saharan dust particles over the basin from MODIS data in the year 2001. Atmospheric Chemistry and Physics 4(9/10): 2367-2391.

Cao, M., M. Zhang, X. Su and L. Wang. 2023: A Two-Stage Machine Learning Algorithm for Retrieving Multiple Aerosol Properties Over Land: Development and Validation. IEEE Transactions on Geoscience and Remote Sensing 61: 1-17.

Ding, H., L. Zhao, S. Liu, X. Chen, G. de Leeuw, F. Wang, F. Zheng, Y. Zhang, J. Liu and J. Li. 2022: FY-4A/AGRI aerosol optical depth retrieval capability test and validation based on NNAeroG. Remote Sensing 14(21): 5591.

Fu, D., H. Shi, C. A. Gueymard, D. Yang, Y. Zheng, H. Che, X. Fan, X. Han, L. Gao and J. Bian. 2024: A deep-learning and transfer-learning hybrid aerosol retrieval algorithm for FY4-AGRI: Development and verification over Asia. Engineering 38: 164-174.

Hilborn, E. D., D. G. Catanzaro and L. E. Jackson. 2012: Repeated holdout cross-validation of model to estimate risk of Lyme disease by landscape characteristics. International journal of environmental health research 22(1): 1-11.

Holben, B. N., T. F. Eck, I. a. Slutsker, D. Tanré, J. Buis, A. Setzer, E. Vermote, J. A. Reagan, Y. Kaufman and T. Nakajima. 1998: AERONET—A federated instrument network and data archive for aerosol characterization. Remote sensing of environment 66(1): 1-16.

Jiang, J., M. Tao, X. Xu, Z. Jiang, W. Man, J. Wang, L. Wang, Y. Wang, Y. Zheng, J. Tao and L. Chen. 2023: A Generalized Aerosol Algorithm for Multi‐Spectral Satellite Measurement With Physics‐Informed Deep Learning Method. Geophysical Research Letters 50(24).

Jiang, X., Y. Xue, C. Jin, R. Bai, Y. Sun and S. Wu. 2022: A simple band ratio library (BRL) algorithm for retrieval of hourly aerosol optical depth using FY-4A AGRI geostationary satellite data. Remote Sensing 14(19): 4861.

Legg, S., 2021: IPCC, 2021: Climate change 2021-the physical science basis. Interaction 49(4): 44-45.

Levy, R. C., L. A. Remer and O. Dubovik. 2007: Global aerosol optical properties and application to Moderate Resolution Imaging Spectroradiometer aerosol retrieval over land. Journal of Geophysical Research: Atmospheres 112(D13).

Lu, F., X.-H. Zhang, B.-Y. Chen, H. Liu, R. Wu, Q. Han, X. Feng, Y. Li and Z. Zhang. 2017: FY-4 geostationary meteorological satellite imaging characteristics and its application prospects. J. Mar. Meteorol 37(2): 1-12.

Lundberg, S. M. and S.-I. Lee. 2017: A unified approach to interpreting model predictions. Advances in neural information processing systems 30.

Min, M., C. Wu, C. Li, H. Liu, N. Xu, X. Wu, L. Chen, F. Wang, F. Sun and D. Qin. 2017: Developing the science product algorithm testbed for Chinese next-generation geostationary meteorological satellites: Fengyun-4 series. Journal of Meteorological Research 31(4): 708-719.

She, L., H. K. Zhang, Z. Li, G. de Leeuw and B. Huang. 2020: Himawari-8 aerosol optical depth (AOD) retrieval using a deep neural network trained using AERONET observations. Remote Sensing 12(24): 4125.

Si, Y., L. Gao, L. Chen, Q. Tan, X. Zhang, B. Li, H. Yan, X. Zhang, F. Lu and X. Zhang. 2024: An adaptive dark-target algorithm for retrieving land AOD applied to FY-4B/AGRI data. IEEE Journal of Selected Topics in Applied Earth Observations and Remote Sensing.

Su, X., L. Wang, M. Cao, L. Yang, M. Zhang, W. Qin, Q. Cao, Y. Yang and L. Li. 2023: Fengyun 4A land aerosol retrieval: Algorithm development, validation, and comparison with other datasets. IEEE Transactions on Geoscience and Remote Sensing 61: 1-16.

Tao, M., L. Chen, Z. Wang, J. Tao, H. Che, X. Wang and Y. Wang. 2015: Comparison and evaluation of the MODIS Collection 6 aerosol data in China. Journal of Geophysical Research: Atmospheres 120(14): 6992-7005.

Vaswani, A., N. Shazeer, N. Parmar, J. Uszkoreit, L. Jones, A. N. Gomez, Ł. Kaiser and I. Polosukhin. 2017: Attention is all you need. Advances in neural information processing systems 30.

Wang, H., M. Fan, S. Jiao, H. Yan, B. Xu, X. Liu, Y. Wang, J. Tao and L. Chen. 2025: An Improved Aerosol Retrieval Algorithm for FY-4A/AGRI Data Based on the GRASP Framework. IEEE Transactions on Geoscience and Remote Sensing.

Wei, J., Z. Wang, Z. Li, Z. Li, S. Pang, X. Xi, M. Cribb and L. Sun. 2024: Global aerosol retrieval over land from Landsat imagery integrating Transformer and Google Earth Engine. Remote Sensing of Environment 315: 114404.

Wei, X., N.-B. Chang, K. Bai and W. Gao. 2020: Satellite remote sensing of aerosol optical depth: Advances, challenges, and perspectives. Critical Reviews in Environmental Science and Technology 50(16): 1640-1725.

Xu, M., Y. Bao, D. Xu, Q. Lu and X. Zhang. 2020: Retrieval of aerosol optical depth based on FY-4A satellite data and its analysis and application. China Environmental Science 40(12): 5162-5168.

Yang, J., Z. Zhang, C. Wei, F. Lu and Q. Guo. 2017: Introducing the new generation of Chinese geostationary weather satellites, Fengyun-4. Bulletin of the American Meteorological Society 98(8): 1637-1658.

Yanqing, X., L. Zhengqiang and H. Weizhen. 2022: Aerosol optical depth retrieval over land using data from AGRI onboard FY-4A. National Remote Sensing Bulletin 26(5): 913-922.

Yoshida, M., M. Kikuchi, T. M. Nagao, H. Murakami, T. Nomaki and A. Higurashi. 2018: Common retrieval of aerosol properties for imaging satellite sensors. Journal of the Meteorological Society of Japan. Ser. II.

Zhang, J. and J. S. Reid. 2006: MODIS aerosol product analysis for data assimilation: Assessment of over‐ocean level 2 aerosol optical thickness retrievals. Journal of Geophysical Research: Atmospheres 111(D22).

Zhou, D., Q. Wang, S. Li and J. Yang. 2024: Preliminary Retrieval and Validation of Aerosol Optical Depths from FY-4B Advanced Geostationary Radiation Imager Images. Remote Sensing 16(2): 372.